

## Zwitterionic Metalates of Group 11 Elements and Their Use as Metalloligands for the Assembly of Multizwitterionic Clusters

Roberto Pattacini, Lorenzo Barbieri, Alessandro Stercoli, Daniele Cauzzi,\*  
Claudia Graiff, Maurizio Lanfranchi, Antonio Tiripicchio, and Lisa Elviri

Contribution from the Dipartimento di Chimica Generale ed Inorganica, Chimica Analitica,  
Chimica Fisica, Università di Parma, Parco Area delle Scienze 17/A, I-43100 Parma, Italy

Received August 17, 2005; E-mail: cauzzi@unipr.it

**Abstract:** Reaction of RNHC(S)PPh<sub>2</sub>NPPh<sub>2</sub>C(S)NR (HRSNS; R = Me, Et) with M<sup>I</sup> (M = Cu, Ag, Au) salts afforded zwitterionic complexes of the general formula [M(RSNS)] (M = Cu, Ag, Au). The ligand was found in the solid state in *S,S*-κ<sup>2</sup> and *S,N,S*-κ<sup>3</sup> coordination fashions. [Cu(RSNS)] and [Ag(RSNS)] can be used as metalloligand building blocks for the assembly of pentanuclear multizwitterionic Cu<sub>5</sub>, Cu<sub>3</sub>Ag<sub>2</sub> and Ag<sub>5</sub> core clusters of the general formula [M'<sub>2</sub>{M(RSNS)}<sub>3</sub>]<sup>2+</sup> (M = Cu, M' = Cu, Ag; M = M' = Ag) upon reaction with suitable M' salts. The crystal structures of the most significant compounds are reported herein. Compound [Ag<sub>2</sub>{Ag(RSNS)}<sub>2</sub>(OTf)<sub>2</sub>] was also isolated and structurally characterized, representing a model for the intermediate species of the aforementioned assembly.

### Introduction

Zwitterionic compounds are defined by the on-line IUPAC Compendium of Chemical Terminology<sup>1</sup> as “Neutral compounds having formal unit electrical charges of opposite sign”. However, zwitterionic metal complexes need a more detailed description, which has been given by Remi Chauvin in his review concerning zwitterionic organometalates.<sup>2</sup> Indeed, couples of opposite charges may be easily evidenced in the Lewis structures although it is often possible to define resonance forms in which all the atoms are neutral. In this case the molecule cannot be called *zwitterion*. In addition, single positive and negative charges can be delocalized over a group of atoms, as carboxylate groups in amino acids and betaines.

Single, nonpolymeric, neutral molecules containing more than one charge couple<sup>3</sup> may be generally called “multizwitterions,” different from polyzwitterions, which refers to polymers containing zwitterionic chain substituents.<sup>4</sup> If further positive or negative charges are present, ionic molecules can be called zwitterion-cations or zwitterion-anions in order to distinguish them from ordinary ions.<sup>5</sup>

As a consequence of the charge separation, a very strong molecular electric dipole moment is observed depending on the distance between the charges barycenters. This strong dipole and amphiphilicity allow these “neutral ions” to be applied in a wide range of fields. Molecular zwitterions or zwitterionic polymers are studied as stationary phases<sup>6</sup> or eluents<sup>7</sup> in liquid

chromatography, as drugs,<sup>8</sup> and as NLO chromophores.<sup>9</sup> As far as zwitterionic coordination compounds are concerned, their most important and outstanding application is in metallocene-catalyzed Ziegler–Natta polymerization<sup>10</sup> or even as carriers for membranes.<sup>11</sup>

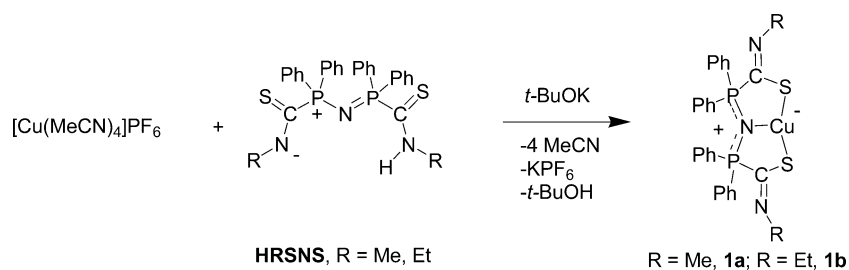
Zwitterionic metal complexes can be prepared following different strategies, the most common being as follows: (a) by reaction of zwitterionic ligands with metal species<sup>12</sup> (this is also the case of the compounds presented in this paper); (b) by generating the charge separation upon coordination;<sup>13</sup> and (c) by association of a positive (or negative) metal center with an oppositely charged ligand maintaining the charge separation.<sup>14</sup> In addition, zwitterionic complexes can be divided in two main categories; the most common one regroups complexes in which the metal center bears the formal positive charge, while the second comprises the still uncommon “zwitterionic metalates” whose metal center is formally negative.

Recently, the reaction between Ph<sub>2</sub>PNHPPH<sub>2</sub> (dppa) and isothiocyanates was reported by our group.<sup>15</sup> Reaction of dppa with EtNCS afforded the new zwitterionic ligand EtNC(S)Ph<sub>2</sub>-PNPPh<sub>2</sub>C(S)NHEt (HEtSNS). Depending on the reaction condi-

(1) www.iupac.org/publications/compendium/index.html.  
(2) Chauvin, R. *Eur. J. Inorg. Chem.* **2000**, 4, 577–591.  
(3) (a) Finnen, D. C.; Pinkerton, A. A.; *Acta Crystallogr.* **1997**, C53, 1455–1457. (b) Karame, I.; Tommasino, M. L.; Faure, R.; Fenet, B.; Lemaire, M. *Chem. Lett.* **2004**, 33 (2), 178–179.  
(4) Lowe, A. B.; McCormick, C. L. *Chem. Rev.* **2002**, 102 (11), 4177–4189.  
(5) Gudat, D. *Top. Curr. Chem.* **2004**, 232, 175–212.  
(6) Nesterenko, P. N.; Haddad, P. R. *Anal. Sci.* **2000**, 16 (6), 565–574.  
(7) Yan, Z.; Yanyan, L.; Fritz, J. S.; Haddad, P. R. *J. Chromatogr., A* **2003**, 1020 (2), 259–264.

(8) Pagliara, A.; Carrupt, P.-A.; Caron, G.; Gaillard, P.; Testa, B. *Chem. Rev.* **1997**, 97, 3385–3400.  
(9) (a) Geskin, V. M.; Lambert, C.; Bredas, J.-L. *J. Am. Chem. Soc.* **2003**, 125 (50), 15651–15658. (b) Lambert, C.; Stadler, S.; Bourhill, G.; Bräuchle, C. *Angew. Chem., Int. Ed. Engl.* **1996**, 35 (6), 644–646.  
(10) (a) Piers, W. E. *Chem.–Eur. J.* **1998**, 4 (1), 13–18. (b) Gerhard, E. *Chem. Commun.* **2003**, 13, 1469–1476. Strauch, J. W.; Erker, G.; Kehr, G.; Fröhlich, R. *Angew. Chem., Int. Ed.* **2002**, 41, 2543–2546.  
(11) Lee, H.; Kim, D. B.; Kim, S.-H.; Kim, H. S.; Kim, S. J.; Choi, D. K.; Kang, Y. S.; Won, J. *Angew. Chem., Int. Ed.* **2004**, 43 (23), 3053–3056.  
(12) Galindo, A.; Miguel, D.; Perez, J. *Coord. Chem. Rev.* **1999**, 193, 643–690.  
(13) Schmidbaur, H. *Angew. Chem., Int. Ed.* **1983**, 22, 907–927.  
(14) (a) Ronig, B.; Schulze, H.; Pantenburg, I.; Wesemann, L. *Eur. J. Inorg. Chem.* **2005**, (2), 314–320. (b) Thomas, J. C.; Peters, J. C. *J. Am. Chem. Soc.* **2003**, 125 (29), 8870–8888.  
(15) Asti, M.; Cammi, R.; Cauzzi, D.; Graiff, C.; Pattacini, R.; Predieri, G.; Stercoli, A.; Tiripicchio, A. *Chem.–Eur. J.* **2005**, 11, 3413–3419.

## Scheme 1



tions, other products were also identified and structurally characterized. HEtSNS contains the zwitterionic functional group  $P^+C(S)N^-$  whose coordinating properties were never studied before. Its first completely characterized complex [(EtSNS)Rh(CO)] is a zwitterionic metalate in which the zwitterion-anion EtSNS<sup>-</sup> acts as an *S,N,S-κ<sup>3</sup>* ligand. This complex bears a high dipole moment, calculated by DFT methods up to 17 D. Indeed, the computation showed that the positive charge is mainly delocalized over the two P atoms, whereas the negative one is distributed on the Rh–N system.

In this paper, the preparation of new zwitterionic metalates of Cu, Ag, and Au is described. These complexes were also used as bidentate metalloligand building blocks for the rational assembly of multizwitterionic clusters, whose structures, determined by X-ray diffraction, are reported and show interesting features.

## Results and Discussion

**Reactions of RNHC(S)PPh<sub>2</sub>NPPh<sub>2</sub>C(S)NR (HRSNS; R = Me, Et) with M<sup>I</sup> Group 11 Species.** Reaction of [Cu(MeCN)<sub>4</sub>][PF<sub>6</sub>] with HRSNS in a 1:1 molar ratio afforded [Cu(RSNS)] (R = Me, **1a**; R = Et, **1b**) in quantitative yields (Scheme 1, charge locations have *formal* character). A more convenient synthetic route implies the use of CuCl, although a lower yield is obtained. Deprotonation of HRSNS was achieved using *t*-BuOK, forming in both cases insoluble potassium salts and *t*-BuOH.

Complex **1b** was structurally characterized by X-ray diffraction methods (Figure 1; for clarity, the atoms are depicted as spheres. Ortep views of the crystal structures of all the compounds with thermal ellipsoids are reported in the Supporting Information) and displayed a crystallographically imposed *C*<sub>2</sub> symmetry, the 2-fold axis passing through the Cu1 and N1 atoms.

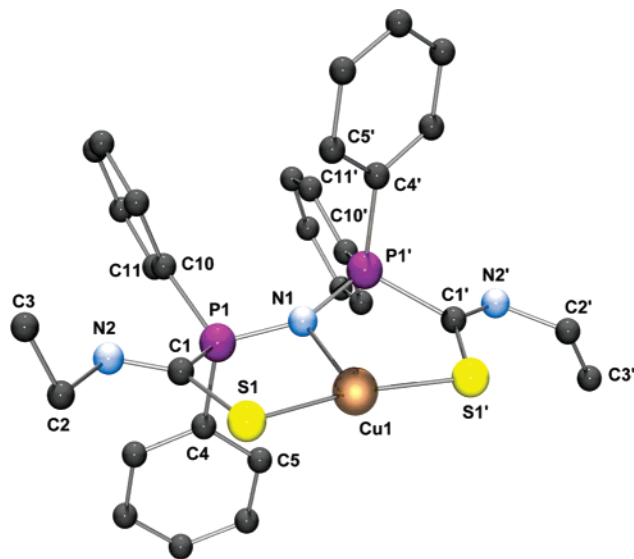
The metal is coordinated in a distorted T-shaped geometry [S1–Cu1–S1' = 167.88(5)°] through S1, S1', and N1. The PNP system maintains geometric parameters comparable to those found for the free ligand [P1–N1 distance, 1.581(2) Å; P1–N1–P1' angle, 143.6(2)°]. N1 adopts a planar geometry, being the sum of the bond angles 360°. The S1–C1 bond length is typical for C–S single bonds, while the N2–C1 one suggests a double bond character.

Complexes **1a** and **1b** can be well compared with [(EtSNS)Rh(CO)]<sup>15</sup> and therefore considered as zwitterionic metalates. The formal negative and positive charges are located over the copper and the two phosphorus atoms, respectively. The two fused penta-atomic Cu, S, C, P, N rings are formed by five different atoms. The [–Ph<sub>2</sub>PNPPh<sub>2</sub>–]<sup>+</sup> cationic group can be associated with the classical [Ph<sub>3</sub>PNPPh<sub>3</sub>]<sup>+</sup> cation (PPN<sup>+</sup>).

Indeed, as evidenced by the bent geometry of the P–N–P group of PPN<sup>+</sup>, the nitrogen may *potentially* coordinate a metal center through the N atom lone pair, even though it has never been found coordinating. In the case of the RSNS<sup>-</sup> complexes, the [–Ph<sub>2</sub>PNPPh<sub>2</sub>–]<sup>+</sup> coordination is forced by the *S,S* chelation that brings N1 in the good geometry. The weak character of the Cu–N bond can be deduced from the Cu–N [2.199(3) Å] and Cu–S [2.158(2) Å] bond lengths, respectively, notably longer and shorter than those typically observed for Cu<sup>I</sup> species.

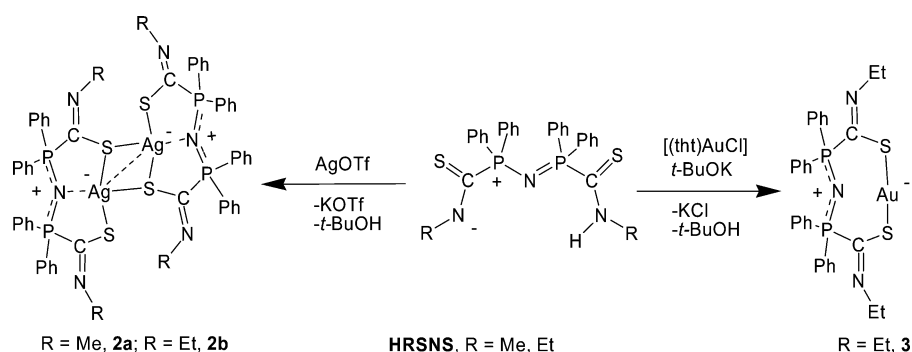
The aforementioned reaction has been extended to Ag(I) and Au(I) (Scheme 2). Reaction of HRSNS with AgOTf and *t*-BuOK (OTf<sup>-</sup> = CF<sub>3</sub>SO<sub>3</sub><sup>-</sup>) afforded complexes [Ag(RSNS)] (R = Me, **2a**; R = Et, **2b**) in quantitative yields. Compound **2a** was structurally characterized by X-ray diffraction methods and was found to crystallize as a dimer. In the crystals two crystallographic independent molecules (A and B) are found lying on symmetry centers. A view of the crystal structure of one of the two independent molecules (A) is given in Figure 2. A comparison between the crystallographic geometric parameters of the two independent molecules is reported in Table 1.

The ligand coordinates to the metal centers through the sulfur atoms, found one in terminal and one in bridging modality, in such a way that a four-membered planar Ag<sub>2</sub>S<sub>2</sub> ring is formed. The S1–Ag1–S2 angles [137.08(9)° for molecule A, 136.2(1)° for molecule B] are smaller than the analogue S–Cu–S angle in **1b** [167.88(5)°], as a result of the bridging coordination.

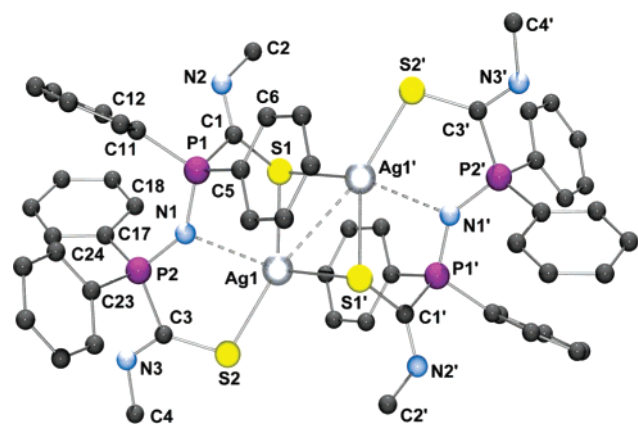


**Figure 1.** View of the crystal structure of complex **1b**. Symmetry transformations ('):  $-x, y, -z + 1/2$ . Selected bond distances (Å) and angles (deg): Cu1–S1 2.158(2), Cu1–N1 2.199(3), P1–N1 1.581(2), P1–C1 1.838(3), S1–C1 1.745(4), N2–C1 1.265(4), S1–Cu1–S1' 167.88(5), S1–Cu1–N1 96.06(3), N1–P1–C1 108.83(2), C1–S1–Cu1 101.69(1), P1'–N1–P1 143.6(2), P1–N1–Cu1, 108.2(1), S1–C1–P1 116.5(2).

Scheme 2

**Table 1.** Selected Bond Distances (Å) and Angles (deg) for Complex **2a** (Crystallographically Independent Molecules A and B)

bond distances (Å) molecule A		bond distances (Å) molecule B	
Ag1–Ag1'	3.125(2)	Ag1–Ag1'	2.997(2)
Ag1–N1	2.635(6)	Ag1–N1	2.721(6)
Ag1–S1	2.576(3)	Ag1–S1	2.438(4)
Ag1–S2	2.462(3)	Ag1–S2	2.566(3)
Ag1–S1'	2.678(3)	Ag1–S1'	2.680(3)
P1–N1	1.566(6)	P1–N1	1.562(6)
P2–N1	1.607(6)	P2–N1	1.607(6)
bond angles (deg) molecule A		bond angles (deg) molecule B	
S1–Ag1–S2	137.08(9)	S1–Ag1–S2	136.2(1)
Ag1–S1–Ag1'	72.98(8)	Ag1–S1–Ag1'	69.65(7)
S2–Ag1–Ag1'	167.39(8)	S2–Ag1–Ag1'	166.34(8)
S2–Ag1–S1'	115.8(1)	S2–Ag1–S1'	113.3(1)
S1–Ag1–S1'	107.02(8)	S1–Ag1–S1'	110.35(7)
N1–Ag1–Ag1'	106.4(1)	N1–Ag1–Ag1'	107.7(1)
P2–N1–P1	139.6(4)	P2–N1–P1	138.5(4)

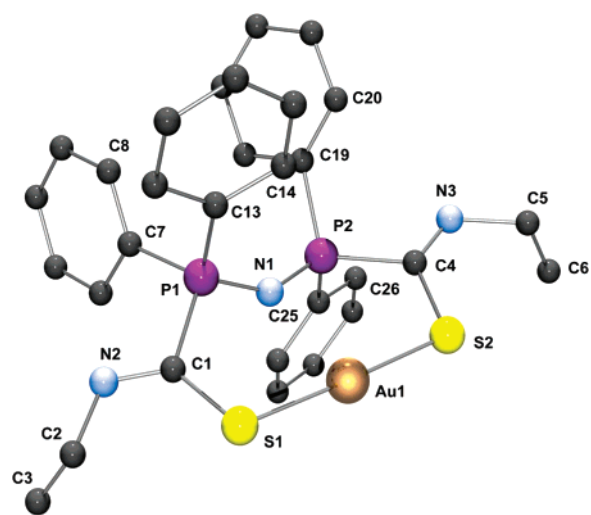
**Figure 2.** View of the crystal structure of complex **2a** (molecule A). Symmetry transformations ( $\hat{\cdot}$ ):  $-x, -y, -z$ .

The two independent molecules show remarkable structural differences. In fact, the Ag1A–Ag1A' distance is longer than the Ag1B–Ag1B' one [3.125(2) and 2.997(2) Å, respectively], while the Ag1A–N1A distance is shorter than the analogue Ag1B–N1B one [2.635(6) Å and 2.721(6) Å, respectively]. Moreover, the distances between Ag1A and Ag1B from the planes defined by P1A, N1A, P2A and P1B, N1B, P2B are 1.271(1) and 1.907(1) Å, respectively. These data indicate that the shorter the Ag...Ag separation, the longer the Ag...N separation (and vice versa); therefore, in complex **2a** the Ag...N interactions may exist. The sum of the bond angles of N1A and N1B (354.74(8)° and 347.49(8)°) differ significantly from

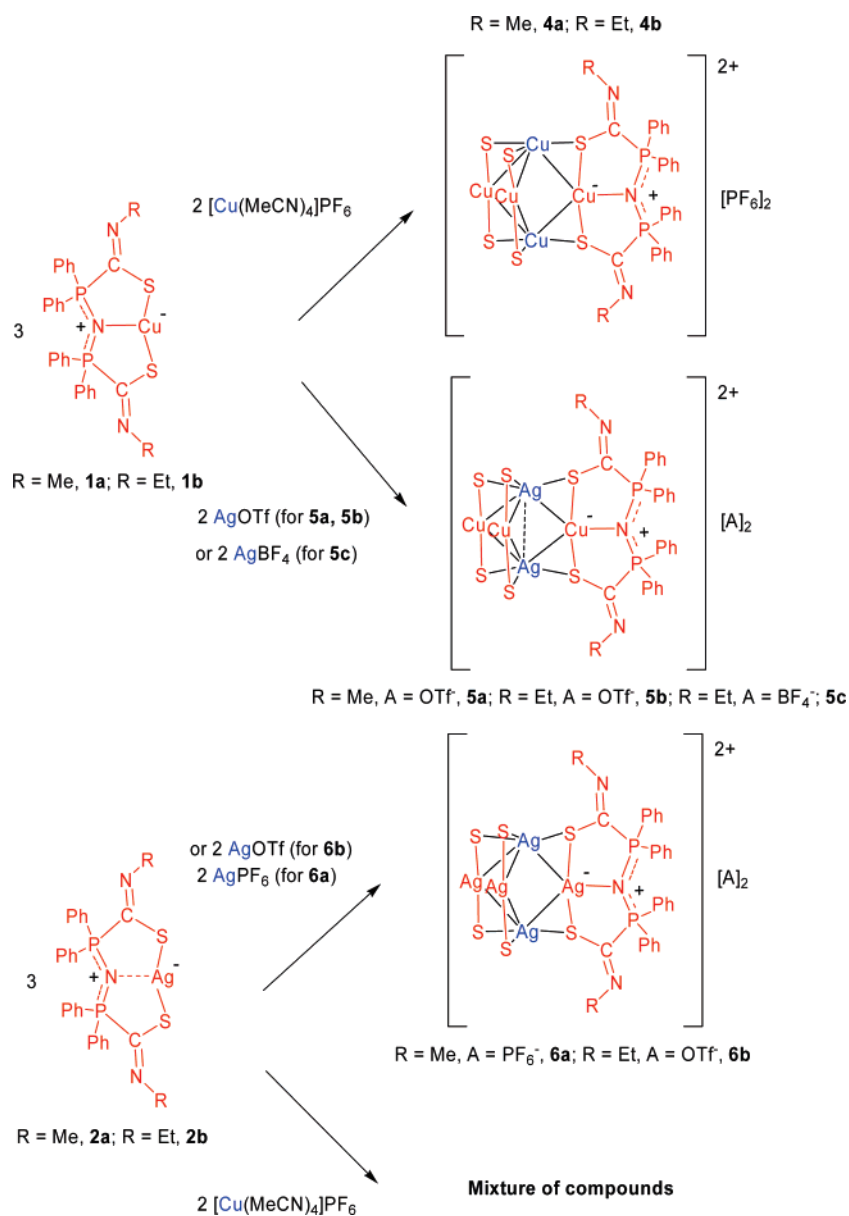
that observed in compound **1b**, indicating a less pronounced  $sp^2$  character for the nitrogen atoms also due to the weaker coordination interaction.

The NMR data suggest that the dimer dissociates in solution at room temperature, as deduced by their  $^{31}\text{P}$  NMR spectra: **2a** and **2b** display a narrow singlet in the typical range for coordinated  $\text{RSNS}^-$ , instead of two signals expected for the dimer. In the  $^1\text{H}$  spectrum, the **2a** methyl groups are equivalent and resonate as doublets with the protons coupled with the closer  $^{31}\text{P}$  nucleus. The methylene groups of **2b** are also equivalent and resonate as a doublet of quartets, being coupled also with the methyl protons. The  $^1\text{H}$  NMR spectra of complex **2b** has been recorded in  $\text{CDCl}_3$  in the temperature range 298–230 K. The methylene and methyl group signals broadened at low temperatures, but no further signals were observed down to 230 K (the methylene group signal at different temperatures has been reported in the Supporting Information).

Reaction of  $[(\text{tth})\text{AuCl}]$  (tth = tetrahydrothiophene) with HEtSNS and  $t\text{-BuOK}$  afforded compound  $[\text{Au}(\text{EtSNS})]$  (**3**), whose crystal structure is shown in Figure 3. In the crystal structure of complex **3** the anion  $\text{EtSNS}^-$  chelates the metal center through the two sulfur atoms in an  $S,S\text{-}\kappa^2$  fashion. The coordination is almost linear [ $\text{S2–Au1–S1}$ , 177.73(6)°;  $\text{Au1–S2}$ , 2.280(2) Å;  $\text{Au1–S1}$ , 2.290(2) Å] and gives rise to an eight-

**Figure 3.** View of the crystal structure of complex **3**. Selected distances (Å) and angles (deg): Au1–S2 2.280(2), Au1–S1 2.290(2), S1–C1 1.759(6), S2–C4 1.764(6), P1–N1 1.584(4), P2–N1 1.582(4), P1–C1 1.848(5), P2–C4 1.858(5), N2–C1 1.265(6), N3–C4 1.255(6); S2–Au1–S1 177.73(6), C1–S1–Au1 102.9(2), C4–S2–Au1 105.8(2), N1–P1–C1 109.8(2), N1–P2–C4 114.3(2), P2–N1–P1 144.0(3), S1–C1–P1 118.9(3), S2–C4–P2 121.6(3).

Scheme 3



membered chelation ring. The Au1...N1 distance is 2.693(4) Å, indicating the absence of an interaction between the two atoms, as confirmed by the distance of Au1 from the plane defined by P1, N1, and P2 [2.023(1) Å]; the sum of the angles [P1–N1–P2, Au1...N1–P1, and Au1...N1–P2] around N1 is 347.04(5)°, similar to that observed for N1B of compound **2**. Complex **3** can be considered a classical 14-electron linear AuL<sub>2</sub> complex. On the other hand, linear Au<sup>I</sup> chelates displaying a 180° bite angle are rather rare, most involving diphosphine and polysulfide ligands and being, to the best of our knowledge, all ionic.<sup>16</sup>

In the crystal packing, probably due to the dipole moment, complexes **1b** and **3** adopt a head to tail disposition, as observed for [(EtSNS)Rh(CO)].<sup>15</sup> Molecules all oriented in the same direction are disposed in layers. Adjacent layers contain molecules with opposite orientations.

(16) (a) Chan, W.-H.; Mak, T. C. W.; Che, C.-M. *J. Chem. Soc., Dalton Trans.* **1998**, 2275–2276. (b) Heuer, B.; Pope, S. J. A.; Reid, G. *Polyhedron* **2000**, *19*, 743–749. (c) Gibson, A. M.; Reid, G. *J. Chem. Soc., Dalton Trans.* **1996**, 1267–1274.

Complexes **1**, **2**, and **3** are soluble in most organic solvents, from low polar toluene to methanol but not in water or hydrocarbons.

**Assembly of [Cu(RSNS)] and [Ag(RSNS)] in Multizwitterionic Clusters.** The mononuclear complexes **1a**, **1b** and **2a**, **2b** behave as metalloligands. The negative charge density on the S–M–S groups induces reactivity toward metal cations. Indeed, addition of M<sup>I</sup> species (M = Ag, Cu) resulted in the assembly of multinuclear cationic clusters with formation of sulfur bridges. The 3:2 reactions of complexes **1a** and **1b** with suitable Cu<sup>I</sup> or Ag<sup>I</sup> salts afforded quantitatively [Cu<sub>2</sub>{Cu(RSNS)}<sub>3</sub>][PF<sub>6</sub>]<sub>2</sub> (R = Me, **4a**; R = Et, **4b**) and [Ag<sub>2</sub>{Cu(RSNS)}<sub>3</sub>][A]<sub>2</sub> (R = Et, A = OTf<sup>-</sup>, **5a**; R = Me, A = OTf<sup>-</sup>, **5b**; R = Et, A = BF<sub>4</sub><sup>-</sup>, **5c**), respectively, as shown in Scheme 3 (for clarity, only one of the three ligands is completely depicted; for the other two, only the sulfur atoms are evidenced). In the same way, complexes **2a** and **2b** reacted with suitable Ag<sup>I</sup> salts yielding [Ag<sub>2</sub>{Ag(RSNS)}<sub>3</sub>][A]<sub>2</sub> (R = Me, A = PF<sub>6</sub><sup>-</sup>, **6a**; R = Et, A = OTf<sup>-</sup>, **6b**). Reaction of complexes **2a** and **2b**

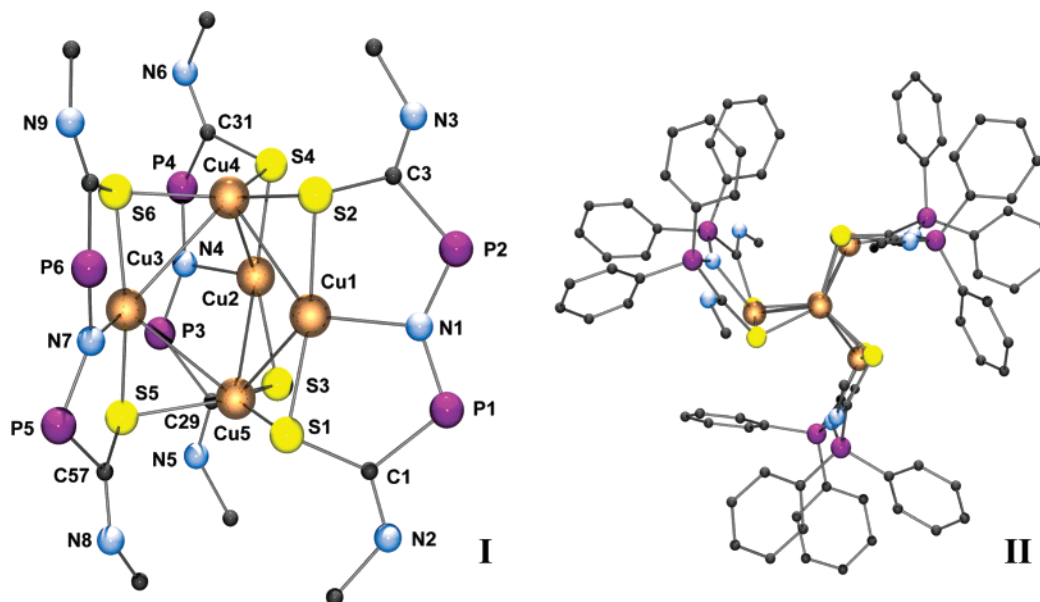


**Figure 4.** Views of the crystal structure of the **4a** cation. Phenyls omitted in structure I. View along the Cu4–Cu5 line in structure II. Selected bond lengths [Å] and angles [deg]: Cu1–Cu5 2.893(1), Cu1–Cu4 2.904(1), Cu2–Cu5 2.846(1), Cu2–Cu4 2.887(1), Cu3–Cu5 2.841(1), Cu3–Cu4 2.891(1), Cu1–N1 2.163(5), Cu2–N4 2.178(5), Cu3–N7 2.185(5), Cu1–S1 2.195(2), Cu1–S2 2.195(2), Cu2–S3 2.189(2), Cu2–S4 2.190(2), Cu3–S6 2.181(2), Cu3–S5 2.194(2), Cu4–S2 2.273(2), Cu4–S4 2.301(2), Cu4–S6 2.237(2), Cu5–S3 2.258(2), Cu5–S1 2.276(2), Cu5–S5 2.298(2); Cu5–Cu1–Cu4 82.48(4), Cu5–Cu2–Cu4 83.62(4), Cu5–Cu3–Cu4 83.64(4), Cu2–Cu4–Cu3 77.00(4), S2–Cu1–S1 165.58(8), S3–Cu2–S4 159.95(8), S6–Cu3–S5 162.14(8).

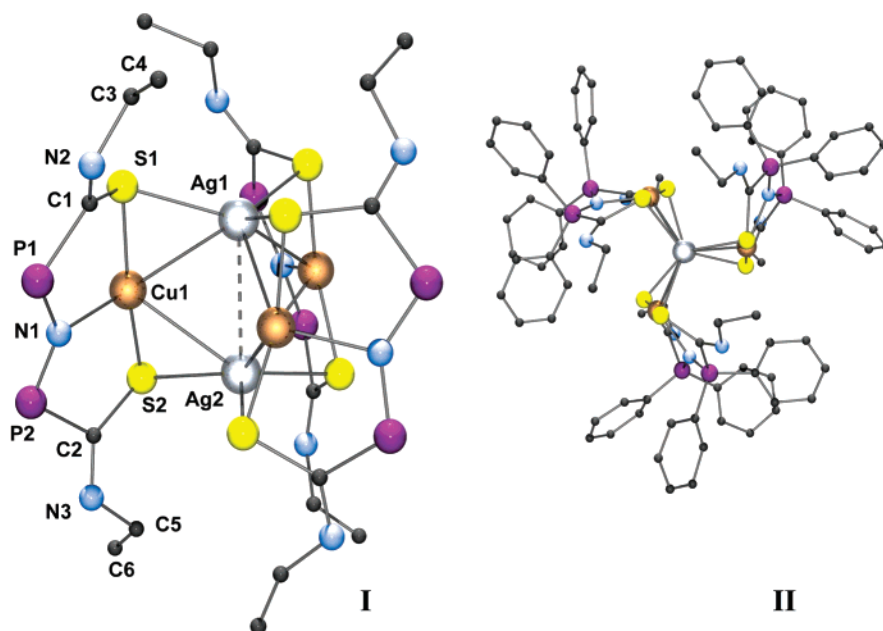


**Figure 5.** Views of the crystal structure of the **5c** cation. Phenyls omitted in structure I. View along the Ag1–Ag2 line in structure II. Selected bond lengths [Å] and angles [deg]: Ag1–S1 2.522(7), Ag1–Cu1 2.882(6), Ag1–Ag2 3.149(7), Ag2–S2 2.512(7), Ag2–Cu1 2.916(6), Cu1–N1 2.162(8), Cu1–S1 2.180(5), Cu1–S2 2.176(5); Ag2–Cu1–Ag1 65.78(19), S1–Cu1–S2 166.57(9). Symmetry transformations ('):  $-y, x - y, z$ ; (''')  $-x + y, -x, z$ .

with  $[\text{Cu}(\text{MeCN})_4]\text{PF}_6$  did not give the expected  $[\text{Cu}_2\{\text{Ag}(\text{RSNS})\}_3][\text{PF}_6]_2$  clusters.

Single crystals of compound **4a**, **5c**, **6a** were obtained, permitting their crystal structure determination. They are ionic compounds; the cation is formed by three  $[\text{M}(\text{RSNS})]$  units joined together by two  $\text{M}'$  atoms ( $\text{M} = \text{M}' = \text{Cu}$  for **4a**,  $\text{M} = \text{Cu}$ ,  $\text{M}' = \text{Ag}$  for **5c**,  $\text{M} = \text{M}' = \text{Ag}$  for **6a**). The metal centers define a trigonal bipyramidal  $\text{M}_3\text{M}'_2$  core, with the  $\text{M}'$  atoms in the axial positions. In the crystals of cluster **6a**, two crystallographic independent molecules were present, displaying analogous structures, while the cation of cluster **5c** adopts a

crystallographically imposed  $\text{C}_3$  symmetry, the axis passing through Ag1 and Ag2.

Looking at the formal charge distribution, they can be regarded as trizwitterionic, dicationic pentanuclear clusters. Views of the crystal structures of clusters **4a**, **5c**, and **6a** are depicted in Figures 4, 5, and 6, respectively (anions omitted for clarity).

For all the three structures, the ligand's sulfur atoms bridge the  $\text{M}'\text{--M}$  bonds. Each nitrogen of the P–N–P groups coordinates to an M atom. All the  $[\text{M}(\text{RSNS})]$  unities are tilted in the same direction with respect to the relative  $\text{M}'$ , M,  $\text{M}'$

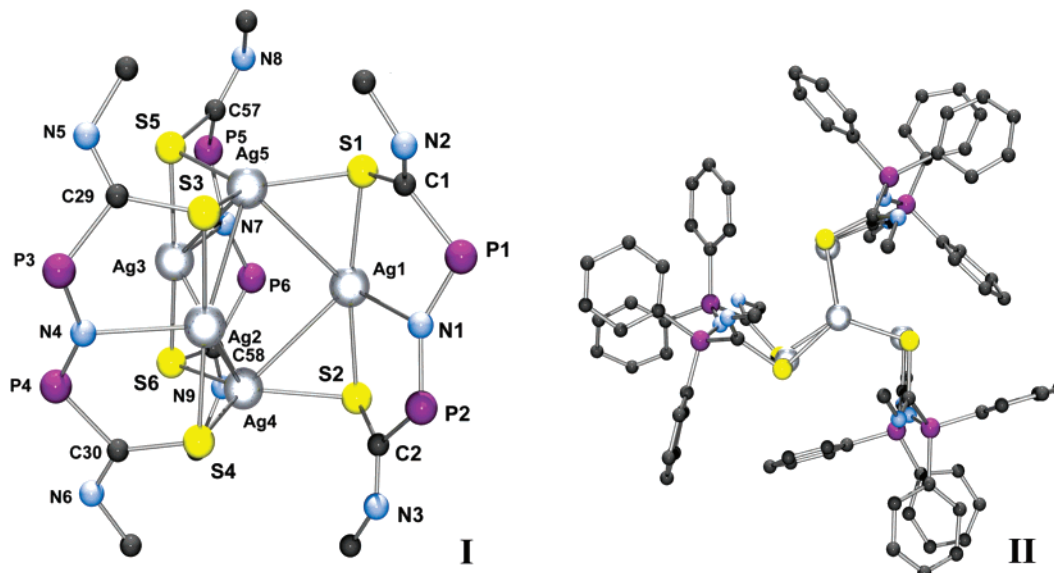


**Figure 6.** Views of the crystal structure of the **6a** cation (crystallographically independent molecule A). Phenyls omitted in structure I. View along the Ag4–Ag5 line in 6II. Selected bond lengths [Å] and angles [deg] (for molecule B are given in square brackets): Ag5–Ag1 3.0539(17) [3.149(2)], Ag5–Ag2 3.1092(12) [3.0603(14)], Ag5–Ag3 3.2386(16) [3.1872(12)], Ag4–Ag3 3.0453(14) [3.0818(17)], Ag4–Ag1 3.1574(12) [3.1230(12)], Ag4–Ag2 3.220(2) [3.2282(14)], Ag5–S1 2.461(3) [2.464(3)], Ag5–S5 2.468(3) [2.468(3)], Ag5–S3 2.489(3) [2.484(3)], Ag4–S4 2.459(3) [2.500(3)], Ag4–S2 2.474(3) [2.481(3)], Ag4–S6 2.486(3) [2.445(3)], Ag1–S1 2.410(3) [2.405(3)], Ag1–S2 2.412(3) [2.390(3)], Ag2–S3 2.402(3) [2.392(3)], Ag2–S4 2.415(3) [2.373(3)], Ag3–S5 2.387(3) [2.400(3)], Ag3–S6 2.408(3) [2.382(3)], Ag1–N1 2.523(6) [2.550(6)], Ag2–N4 2.524(6) [2.503(6)], Ag3–N7 2.484(6) [2.520(7)]; Ag5–Ag1–Ag4 88.59(3) [87.48(3)], Ag5–Ag2–Ag4 86.52(3) [87.14(4)], Ag4–Ag3–Ag5 87.27(4) [87.51(3)], S1–Ag1–S2 168.83(9) [170.42(9)], S3–Ag2–S4 171.98(9) [170.14(9)], S5–Ag3–S6 170.90(9) [170.94(9)].

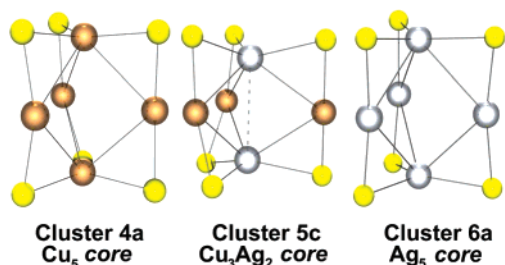


**Figure 7.** Comparison between the *cores* of the **4a**, **5c**, and **6a** cations.

**Table 2.** Comparison between Selected Distances and Angles in Clusters **4a**, **5c**, and **6a**

	4a	5c	6a
M'...M' (Å)	3.821(1)	3.149(7)	4.337(2)
average M–M' (Å)	2.877(1)	2.899(6)	3.138(1)
average M'–M–M' (deg)	83.25(4)	65.8(2)	87.42(3)
average M–M'–M (deg)	80.65(4)	94.8(1)	77.51(3)

plane (Figures 4II, 5II, 6II). The clusters' *core* drawings are reported and compared in Figure 7, and the most important geometric parameters are given in Table 2.

It is noteworthy that the *core* geometry of cluster **5c** differs significantly from cluster **4a** and **6a**. A distortion of the bipyramid is observed, being the two M' axial atoms are much closer. An interaction probably exists between the two Ag atoms, being the Ag...Ag distance is 3.149(7) Å. In consequence, the average M'–M–M' angles are smaller [65.8(2)° for cluster **5c**, 83.25(4)° and 87.42(3)° for cluster **4a** and **6a**, respectively]. The apical metal centers are farther from the plane defined by the three neighbor sulfur atoms [distances from the planes: 0.234(1) and 0.244(1) Å for Cu4 and Cu5, respectively, in **4a**; 0.449(1) and 0.625(2) Å for Ag1 and Ag2 in **5c**, respectively; spanning from 0.198(1) and 0.231(1) Å for **6a**].

Although few examples of Cu<sub>5</sub><sup>17</sup> and Ag<sub>5</sub><sup>18</sup> clusters bearing these types of metal *cores* have been already reported, these are the first cases in which the cage supports positive charges.

Cluster **5c** represents one of the rare examples of complexes displaying an Ag–Cu bond [2.882(6) and 2.916(6) Å for Ag1–Cu1 and Ag2–Cu1]. Surprisingly, molecules containing the Cu–Ag interaction are very rare, whereas Cu–Au and Ag–Au bonds are rather common. To the best of our knowledge, only four structurally defined complexes bearing the aforementioned bond are reported in the literature.<sup>19</sup> A theoretical study is, in our opinion, needed to clarify this observation.

Clusters **4a**, **5c**, and **6a** are stable when exposed to moderate heat, to air, or to light. They can, nevertheless, be disassembled if reacted with anions as CN<sup>−</sup> (fast) or Cl<sup>−</sup> (slower). The apical M<sup>I</sup> ions are subtracted forming the respective salts, and the parent [M(RSNS)] complexes are released.

The formation of **4a**, **4b**, **5a**, **5b**, **5c** and **6a**, **6b** suggested that any combination of M(RSNS) and M<sup>I</sup> (M = Cu, Ag) could lead to the assembly of clusters with desired compositions and geometries. However, the 3:2 reaction of complex [Ag(EtSNS)] (**2b**) with [Cu(MeCN)<sub>4</sub>]PF<sub>6</sub> did not give rise to the expected [Cu<sub>2</sub>{Ag(EtSNS)}<sub>3</sub>][PF<sub>6</sub>]<sub>2</sub> cluster but to a mixture of species, of which [Ag<sub>2</sub>{Cu(EtSNS)}<sub>3</sub>]<sup>2+</sup> resulted as the major one, as

- (17) (a) Dance, I. G. *Chem. Commun.* **1976**, 68–69. (b) Eichhofer, A.; Fenske, D.; Holstein, W. *Angew. Chem.* **1993**, 32, 242–245. (c) Hakansson, M.; Eriksson, H.; Ahman, A. B.; Jagner, S. J. *Organomet. Chem.* **2000**, 595, 102–108. (d) Edwards, P. G.; Gellert, R. W.; Marks, M. W.; Bau, R. J. *Am. Chem. Soc.* **1982**, 104, 2072–2073. (e) Heine, A.; Stalke, D. *Angew. Chem.* **1993**, 32, 121–122.
- (18) (a) Abu-Salah, O. M.; Al-Ohaly, A. R. A.; Mutter, Z. F. *J. Organomet. Chem.* **1990**, 389 (3), 427–34. (b) Bowmaker, G. A.; Tan, L.-C. *Aust. J. Chem.* **1979**, 32 (7), 1443–52.
- (19) (a) Freeman, M. J.; Green, M.; Orpen, A. G.; Salter, I. D.; Stone, F. G. A. *Chem. Commun.* **1983**, 1332–1334. (b) Abu-Salah, O. M.; Hussain, M. S.; Schlemper, E. O. *Chem. Commun.* **1988**, 212–213. (c) Fackler, J. P., Jr.; Lopez, C. A.; Staples, R. J.; Wang, Suning; Winpenney, R. E. P.; Lattimer, R. P. *Chem. Commun.* **1992**, 146–148. (d) Shorrock, C. J.; Xue, B.-Y.; Kim, P. B.; Batchelor, R. J.; Patrick, B. O.; Leznoff, D. B. *Inorg. Chem.* **2002**, 41, 6743–6753.

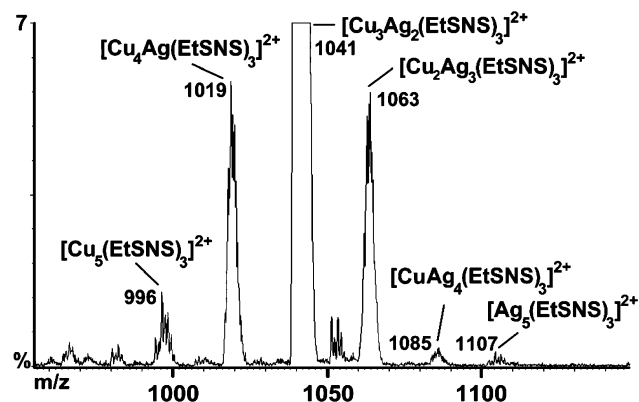


**Figure 8.** ESI-MS spectra of the crude product of the 3:2 reaction between  $[\text{Ag}(\text{EtSNS})]$  (compound **2a**) and  $[\text{Cu}(\text{MeCN})_4][\text{PF}_6]$  in  $\text{CH}_2\text{Cl}_2$ .

detected by ESI-MS analyses and confirmed by means of  $^{31}\text{P}$  NMR spectroscopy. The formation of the cluster with inverted metal ratio ( $\text{Ag}_2\text{Cu}_3$  instead of  $\text{Ag}_3\text{Cu}_2$ ) can be explained by the  $\text{RSNS}^-$  ligand exchange:  $[\text{Ag}(\text{RSNS})] + \text{Cu}^+ = [\text{Cu}(\text{RSNS})] + \text{Ag}^+$ . Several  $[\text{M}_2\{\text{M}'(\text{RSNS})\}_3]^{2+}$  cations ( $\text{M} = \text{Ag}, \text{Cu}$ ;  $\text{M}' = \text{Ag}, \text{Cu}$ ) were detected in the ESI-MS spectrum of the crude product (Figure 8),  $[\text{Ag}_2\{\text{Cu}(\text{EtSNS})\}_3]^{2+}$  (cluster **5b**) being the prevalent one. Together with the  $[\text{Ag}_2\{\text{Cu}(\text{EtSNS})\}_3]^{2+}$  1041  $m/z$  peak (intensity 100), other signals with  $m/z$  1019 and 1063 were observed, respectively correspondent to the  $[\text{Cu}_4\text{Ag}(\text{EtSNS})_3]^{2+}$  and  $[\text{Cu}_2\text{Ag}_3(\text{EtSNS})_3]^{2+}$  ions (relative intensities 6%). Moreover, low intensity peaks 996, 1085, and 1107  $m/z$  were respectively associated with  $[\text{Cu}_5(\text{EtSNS})_3]^{2+}$ ,  $[\text{Ag}_4\text{Cu}(\text{EtSNS})_3]^{2+}$ , and  $[\text{Ag}_5(\text{EtSNS})_3]^{2+}$ . The  $^{31}\text{P}$  NMR spectrum showed several singlets, in the range of coordinating  $\text{EtSNS}^-$  [ $\delta$  13.91 ppm (relative intensity 0.15); 13.79 (0.16); 13.47 (0.28); 13.12 ( $[\text{Ag}_2\{\text{Cu}(\text{EtSNS})\}_3]^{2+}$ , 1); 12.83 (0.14); 12.72 (0.16)]. The most intense signal belonged to  $[\text{Ag}_2\{\text{Cu}(\text{EtSNS})\}_3]^{2+}$  (**5b**), as in the case of the ESI-MS spectrum. The NMR data suggest that the metal scrambling process occurs in solution and seems not induced by the ESI-MS experimental conditions. In addition, cluster **5b** can be isolated in high yields by crystallization. Similar ESI-MS and  $^{31}\text{P}$  NMR spectra were observed in the case of the reaction between complex **1b** and  $\text{AgOTf}$ . In this case, however, the relative intensities of the  $[\text{Ag}_2\{\text{Cu}(\text{EtSNS})\}_3]^{2+}$  signals are much more intense, and the other clusters can be considered as impurities.

The reaction ratio between the complex  $\text{M}(\text{RSNS})$  and the  $\text{M}^{\text{I}}$  ion can be different from 3:2. In fact, reaction of  $[\text{Ag}(\text{EtSNS})]$  (**2b**) with  $\text{AgOTf}$  in a 1:1 molar ratio led quantitatively to the formation of  $[\text{Ag}_2\{\text{Ag}(\text{EtSNS})\}_2(\text{OTf})_2]$  (**7**), a bis-zwitterion. A view of its crystal structure is shown in Figure 9.

In the centrosymmetric crystal structure of complex **7**, the  $\text{Ag}(\text{EtSNS})$  groups are bound to two  $\text{AgOTf}$  groups, the four metal centers forming a planar  $\text{Ag}_4$  ring. The  $\text{Ag}\cdots\text{Ag}$  separations [ $\text{Ag}1\cdots\text{Ag}2'$  3.174(2),  $\text{Ag}1\cdots\text{Ag}2$  3.259(2) Å] suggest metal–metal interactions and are longer than those found in the dimeric crystal structure of complexes **2a** [ $\text{Ag}1-\text{Ag}1'$  3.125(2) and  $\text{Ag}1-\text{Ag}1'$  2.997(2) Å for **2aA** and **2aB**, respectively] and slightly longer than those found for cluster **6** [average  $\text{Ag}-\text{Ag}$  bond length: 3.138(1) Å]. The  $\text{N}1-\text{Ag}1$  distance [2.572(4) Å] is shorter than those found for complex **2b**, while the sulfur atoms bridge two metals almost symmetrically.  $\text{Ag}2$  is finally bound to an oxygen of a triflate ion. The  $\text{N}1-\text{Ag}1$  line form an angle of 111.86(6) with the  $\text{Ag}_4$  plane. The ligand maintains

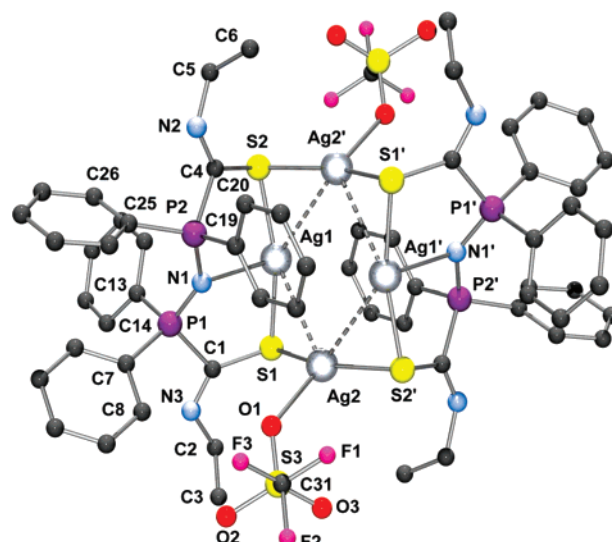


**Figure 9.** View of the crystal structure of compound **7**. Selected bond lengths [Å] and angles [deg]:  $\text{Ag}1\cdots\text{Ag}2'$  3.174(2),  $\text{Ag}1\cdots\text{Ag}2$  3.259(2),  $\text{Ag}1-\text{S}2$  2.405(2),  $\text{S}2-\text{Ag}2'$  2.399(2),  $\text{Ag}1-\text{S}1$  2.416(2),  $\text{Ag}2-\text{S}1$  2.414(2),  $\text{Ag}1-\text{N}1$  2.572(4),  $\text{Ag}2-\text{O}1$  2.465(4),  $\text{Ag}1-\text{Ag}2-\text{Ag}1'$  79.31(3),  $\text{Ag}2-\text{Ag}1-\text{Ag}2'$  100.69(3),  $\text{Ag}2-\text{S}1-\text{Ag}1$  84.87(8),  $\text{Ag}2'-\text{S}2-\text{Ag}1$  82.73(7),  $\text{S}2-\text{Ag}1-\text{S}1$  164.70(7),  $\text{S}2'-\text{Ag}2-\text{S}1$  154.23(6),  $\text{S}2-\text{Ag}1-\text{N}1$  85.89(12),  $\text{S}1-\text{Ag}1-\text{N}1$  86.57(11).

geometrical parameters comparable with those found for the  $\text{RSNS}^-$  species described above. Examples of quasi-planar  $\text{Ag}_4\text{S}_4$  core complexes were already reported in the literature.<sup>20</sup>

When complex **7** is reacted, in a 1 to 1 ratio, with complex **2b**, cluster  $[\text{Ag}_2\{\text{Ag}(\text{EtSNS})\}_3][\text{OTf}]_2$  (**6b**) is quantitatively formed, as depicted in Scheme 4 (for clarity, only one of the three ligand molecules is completely shown for cluster **6**; for the other two, only the S bridging atoms have been evidenced).

Since complex **7** is an intermediate species in the assembly of cluster **6b**, it is possible to hypothesize an analogous planar  $\text{Cu}_4$  intermediate in the formation of **4a** and **4b** and  $\text{Cu}_2\text{Ag}_2$  ones for **5a**, **5b**, **5c**. In the case of silver, the coordinating triflate anion may stabilize the tetranuclear species, allowing its isolation. Cluster **6b** can be thus assembled following three different strategies: (a) 5:3 reaction of  $\text{AgOTf}$  with  $\text{HEtSNS}$  in the presence of a base such as *t*-BuOK, (b) 3:2 reaction of complex **2b** with  $\text{AgOTf}$ , and (c) 1:1 reaction of complex **6b** with complex **2b**.

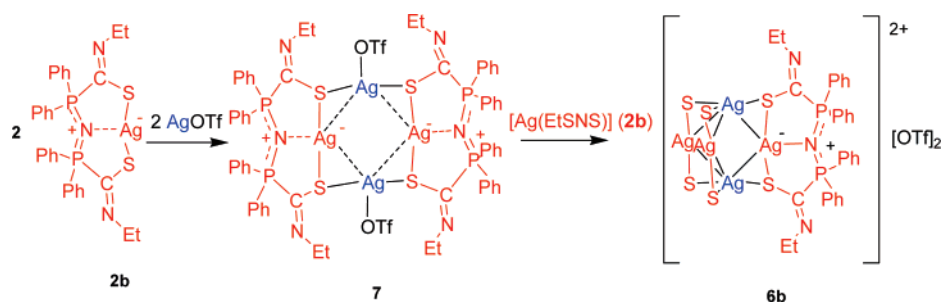
Preliminary results indicate high Stoke's shift luminescence properties for clusters **4(a, b)** and **5(a, b, c)**. The emission spectrum of a crystalline powder sample of cluster **4b** was recorded under a 380 nm continuous excitation radiation at room temperature and at 10 K. They show rather wide bands (Figure 8 in the Supporting Information) ranging from 550 to 760 nm with a maximum at 653 nm at 10 K and ranging from 550 to 737 nm with a maximum at 637 nm at 298 K.

## Conclusions

Zwitterionic metalates are still uncommon in the literature, and their potential applications in catalysis and material science

(20) (a) Wojnowski, W.; Wojnowski, M.; Peters, K.; Peters, E.-M.; von Schnering, H. G. *Z. Anorg. Allg. Chem.* **1985**, *530*, 79–88. (b) Tang, K.; Aslam, M.; Block, E.; Nicholson, T.; Zubieta J. *Inorg. Chem.* **1987**, *26*, 1488–1497. (c) Fackler J. P. J.; Lopez, C. A.; Staples, R. J.; Wang, S.; Winpenny, R. E. P.; Lattimer, R. P. *Chem. Commun.* **1992**, 146–148. (d) Richter, R.; Dietze, F.; Schmidt, S.; Hoyer, E.; Poll, W.; Mootz, D. Z. *Anorg. Allg. Chem.* **1997**, *623*, 135–140.

Scheme 4



are all to be explored. The presence of an electron-rich metal center can be exploited for instance in catalytic reactions and the very strong molecular electrical dipole in NLO applications. The Cu, Ag, and Au complexes reported in this paper continue the series of HRSNS complexes and show that their properties as metalloligands can be extended to other metals in order to produce a series of rationally assembled multizwitterions. Multizwitterionic molecules such as those reported in this paper can show useful properties due to the presence of strong ordered dipoles and are under study. As an example, complexes **4(a,b)**, **5(a,b,c)**, and **6(a,b)** can be considered a new kind of octupolar molecule<sup>21</sup> where three dipoles are disposed with  $C_3$  symmetry in a tangential, rather than radial, way. The assembly of mono- and bimetallic clusters using complex [Au(EtSNS)] (compound **3**) is under study as the coordination chemistry of HRSNS toward other metals of the transition series.

## Experimental Section

**General Remarks.** *t*-BuOK, EtNCS, MeNCS, AgPF<sub>6</sub>, AgBF<sub>4</sub>, and AgOTf were purchased pure (Aldrich and Fluka) and used as received. [Cu(MeCN)<sub>4</sub>][BF<sub>4</sub>], [Cu(MeCN)<sub>4</sub>][PF<sub>6</sub>],<sup>22</sup> [(tbt)AuCl],<sup>23</sup> and dppa (Ph<sub>2</sub>PNHPh)<sub>2</sub><sup>24</sup> were prepared following the procedures reported in the literature. The solvents (Fluka) were dried and distilled by standard techniques. Elemental (C, H, N, S) analyses were performed on a Carlo Erba EA 1108 instrument. <sup>1</sup>H (300 MHz, CDCl<sub>3</sub>, TMS) and <sup>31</sup>P{<sup>1</sup>H} (161.98 MHz, CDCl<sub>3</sub>, 85%–H<sub>3</sub>PO<sub>4</sub>) NMR spectra were recorded on Bruker spectrometers (Avance 300 and AMX-400, respectively). FTIR spectra were recorded on a Nicolet NEXUS spectrometer. A Quattro LC triple quadrupole instrument (Micromass, Manchester, UK) equipped with an electrospray (ESI) interface and a Masslynx v. 3.4 software (Micromass) was used for ESI-MS data acquisition and processing. The nebulizing gas (nitrogen, 99.999% purity) and the desolvation gas (nitrogen, 99.998% purity) were delivered at a flow rate of 80 and 500 L/h, respectively. ESI-MS analyses were performed by operating the mass spectrometer in positive ion (PI) mode, acquiring mass spectra over the scan range *m/z* 100–2800, using a step size of 0.1 Da and a scan time of 2.7 s. The operating parameters of interface were as follows: source temperature 70 °C, desolvation temperature 70 °C, ESI(+) capillary voltage 3.0 kV, cone voltage 15 V, rf lens 0.3 V. The emission spectra were recorded under 380 nm continuous excitation light using a Spex Fluorolog System. A xenon lamp was used as the source, and the detector was an RCA C31034 photomultiplier. The samples were mounted onto an Air Products closed-cycle helium cryostat. The spectra were measured at room temperature and 10 K.

**Preparation of HRSNS (R = Me, Et).** The synthesis of HRSNS has been improved with respect to that reported previously.<sup>15</sup> A solvent-

free reaction between EtNCS and dppa increased the yield to almost quantitative. Moreover, protonation of the ligand with aqueous HCl permitted us to avoid spontaneous solid-state decomposition in EtNC and EtNHC(S)PPh<sub>2</sub>NP(S)Ph<sub>2</sub>, the chlorhydrate HEtSNS·HCl being more stable than the neutral product.

2 g of dppa (3.9 mmol) were dissolved in 3 mL of RNCS (R = Me, 41.1; R = Et, 34.5 mmol), and the mixture was stirred at 32 °C for 20 min (R = Me) or at 25 °C for 20 min (R = Et). After this time, hexane (30 mL) was added, and a yellow solid formed. This precipitate was in turn filtered and washed with hexane (4 × 20 mL) in order to obtain HRSNS (R = Me, Et) as yellow crystalline powders. HRSNS was identified by comparison of its spectroscopic data with that reported previously.<sup>15</sup> Yield: HRSNS 92%, HMeSNS 49%.

HMeSNS E.A. (%) calcd for C<sub>28</sub>H<sub>27</sub>N<sub>3</sub>P<sub>2</sub>S<sub>2</sub>: N, 7.90; C, 63.26; H, 5.12; S, 12.06. Found: N, 7.88; C, 63.82; H, 5.19; S, 11.95. <sup>1</sup>H NMR (300 MHz, CDCl<sub>3</sub>, 25 °C, δ ppm): 7.7–7.3 (m, 20H; Ph), 3.45 (d, 6H, –CH<sub>3</sub>, <sup>3</sup>J(H–H) = 2.7 Hz), 3.44 (s, 1H; S–H). <sup>31</sup>P{<sup>1</sup>H} NMR (161.98 MHz, CDCl<sub>3</sub>, 25 °C): δ = 7.6 (s).

**Preparation of H<sub>2</sub>EtSNSCl.** HCl (2 mL, 12 M) was added to a solution of HEtSNS (500 mg, 0.90 mmol) in CH<sub>2</sub>Cl<sub>2</sub> (30 mL), and the reaction stirred for 15 min at 25 °C. To the suspension, anhydrous Na<sub>2</sub>SO<sub>4</sub> was added, and the solution was filtered. Evaporation of the solvent gave a pale green-yellow solid. The solid was treated by addition of amounts of MeOH (3 × 5 mL) followed by evaporation. The solid obtained was then washed with toluene (4 × 10 mL), yielding H<sub>2</sub>-EtSNSCl as a yellow-green microcrystalline powder. Yield: 91%. The same procedure yielded H<sub>2</sub>MeSNSCl when HMeSNS was used instead of HEtSNS (500 mg, 0.94 mmol). Yield: 69%. The HMeSNS and H<sub>2</sub>MeSNSCl <sup>1</sup>H NMR spectra are discussed in the Supporting Information.

H<sub>2</sub>EtSNSCl E.A. (%) calcd for C<sub>30</sub>H<sub>32</sub>N<sub>3</sub>ClP<sub>2</sub>S<sub>2</sub>: N, 7.05; C, 60.44; H, 5.41; S, 10.76. Found: N, 6.89; C, 60.53; H, 5.19; S, 10.95. <sup>1</sup>H NMR (300 MHz, CDCl<sub>3</sub>, 25 °C, δ ppm): 12.35 (s, 2H; N–H), 7.54–7.26 (m, 20H; Ph), 4.06 (observed multiplicity: quintet, 4H; –CH<sub>2</sub>–, <sup>4</sup>J(H–P) = <sup>3</sup>J(H, <sup>1</sup>H) = 6.7 Hz), 1.44 (t, 6H, –CH<sub>3</sub>, <sup>3</sup>J(H–H) = 6.7 Hz). <sup>31</sup>P{<sup>1</sup>H} NMR (161.98 MHz, CDCl<sub>3</sub>, 25 °C): δ = 14.2 (s).

H<sub>2</sub>MeSNSCl E.A. (%) calcd for C<sub>28</sub>H<sub>28</sub>N<sub>3</sub>ClP<sub>2</sub>S<sub>2</sub>: N, 7.40; C, 59.20; H, 4.97; S, 11.29. Found: N, 7.33; C, 59.25; H, 4.96; S, 11.37. <sup>1</sup>H NMR (300 MHz, CDCl<sub>3</sub>, 25 °C, δ ppm): 12.67 (s, 1H; N–H), 7.2–7.7 (m, 20H; Ph), 3.44 (d, 6H; –CH<sub>3</sub>, <sup>3</sup>J(H–H) = 3.3 Hz), 2.03 (s, br, 1H, S–H). <sup>31</sup>P{<sup>1</sup>H} NMR (161.98 MHz, CDCl<sub>3</sub>, 25 °C): δ = 14.9 (s).

**Preparation of [Cu(RSNS)] (R = Me, **1a**; R = Et, **1b**).** (a) A solution of HRSNS (112 mg R = Et, 106 mg R = Me; 0.2 mmol) in CH<sub>2</sub>Cl<sub>2</sub> (20 mL) was added to a solution of [Cu(MeCN)<sub>4</sub>][PF<sub>6</sub>] (74 mg, 0.2 mmol) in CH<sub>2</sub>Cl<sub>2</sub> (20 mL), resulting in an orange reaction mixture. *t*-BuOK (22 mg, 0.2 mmol in 5 mL of MeOH) was then added, and the color of the solution changed to pale yellow. Stirring was continued for 30 min. The solvent was evaporated, and the pale yellow powder obtained redissolved in CH<sub>2</sub>Cl<sub>2</sub> (20 mL). KPF<sub>6</sub> was removed via filtration. 10 mL of hexane were added in order to separate a yellow oil, removed by centrifugation. Evaporation of the solvent afforded complexes [Cu(RSNS)] (R = Me, Et; **1a** and **1b**, respectively) as white powders. Yields: **1a** 81%, **1b** 84%.

(21) Viau, L.; Bidault, S.; Maury, O.; Brasselet, S.; Ledoux, I.; Zyss, J.; Ishow, E.; Nakatani, K.; Le Bozec, H. *J. Am. Chem. Soc.* **2004**, *126* (27), 8386–8387.

(22) Kubas, G. J. *Inorg. Synth.* **1979**, *19*, 90–92.

(23) Uson, R.; Laguna, A.; Laguna, M. *Inorg. Synth.* **1989**, *26*, 85.

(24) Bhattacharyya, P.; Woollins, J. D. *Polyhedron* **1995**, *14* (23/24), 3367–88.



(b) A solution of HRSNS (112 mg R = Et, 106 mg R = Me; 0.2 mmol) in CH<sub>2</sub>Cl<sub>2</sub> (20 mL) was added to a suspension of CuCl (20 mg, 0.2 mmol) in CH<sub>2</sub>Cl<sub>2</sub> (20 mL), resulting in an orange reaction mixture. *t*-BuOK (22 mg, 0.2 mmol in 5 mL of MeOH) was in turn added, and the color of the solution changed to pale yellow. After stirring for 2 h, the solvent was removed, and the yellow powder redissolved in CH<sub>2</sub>-Cl<sub>2</sub> (20 mL). KCl was removed by filtration. Addition of hexane (10 mL) gave an oil which was removed by centrifugation. Evaporation of the solvent afforded complexes [Cu(RSNS)] (R = Me, Et; **1a** and **1b**, respectively) as white powders. **1a** 73%, **1b** 69%.

**1a**: E.A. (%) calcd for C<sub>28</sub>H<sub>26</sub>N<sub>3</sub>P<sub>2</sub>CuS<sub>2</sub>: N, 7.07; C, 56.60; H, 4.41; S, 10.79. Found: N, 7.15; C, 56.35; H, 4.67; S, 10.47. <sup>1</sup>H NMR (300 MHz, CDCl<sub>3</sub>, 25 °C, TMS): δ = 7.2–7.5 (m, 20H; Ph), 3.66 (s, br, 6H; –CH<sub>3</sub>). <sup>31</sup>P{<sup>1</sup>H} NMR (161.98 MHz, CDCl<sub>3</sub>, 25 °C): δ 9.2 (s).

**1b**: E.A. (%) calcd for C<sub>30</sub>H<sub>30</sub>N<sub>3</sub>CuP<sub>2</sub>S<sub>2</sub>: N, 6.75; C, 57.91; H, 4.86; S, 10.31. Found: N, 6.65; C, 58.08; H, 4.90; S, 10.22. <sup>1</sup>H NMR (300 MHz, CDCl<sub>3</sub>, 25 °C, TMS): δ = 7.2–7.5 (m, 20H; Ph), 3.8 (q, br, <sup>3</sup>J(H,H) = 6.5 Hz, <sup>4</sup>J(H,P) = 2.8 Hz, 4H; –CH<sub>2</sub>–), 1.22 (t, br, <sup>3</sup>J(H,H) = 6.5 Hz, 6H; –CH<sub>3</sub>); <sup>31</sup>P{<sup>1</sup>H} NMR (161.98 MHz, CDCl<sub>3</sub>, 25 °C, H<sub>3</sub>PO<sub>4</sub>): δ = 7.9 (s).

**Preparation of [Ag(RSNS)] (R = Me, **2a**; R = Et, **2b**)**. A solution of HRSNS (112 mg R = Et, 106 mg R = Me; 0.2 mmol) in CH<sub>2</sub>Cl<sub>2</sub> (20 mL) was added to a solution of AgOTf (51 mg, 0.2 mmol) in THF (20 mL), and the color of the reaction mixture changed to pale brown. *t*-BuOK (22 mg, 0.2 mmol in 5 mL of MeOH) was in turn added, and stirring continued for 2 h. Evaporation of the solvent afforded a pale yellow solid which was redissolved in CH<sub>2</sub>Cl<sub>2</sub> (20 mL). KOTf was removed by filtration. Addition of hexane (10 mL) gave a brown oil which was removed by centrifugation. Evaporation of the solvent yielded complexes [Ag(RSNS)]<sub>2</sub> (R = Me, Et; **2a** and **2b**, respectively) as white powders. Yield: **2a** 74%, **2b** 83%.

**2a**: E.A. (%) calcd for C<sub>56</sub>H<sub>52</sub>N<sub>6</sub>Ag<sub>2</sub>P<sub>4</sub>S<sub>4</sub>: N, 6.58; C, 52.67; H, 4.10; S, 10.04. Found: N, 6.37; C, 52.86; H, 4.36; S, 9.87. <sup>1</sup>H NMR (300 MHz, CDCl<sub>3</sub>, 25 °C, TMS): δ = 7.0–7.4 (m, 20H; Ph), 3.47 (d, 6H, <sup>4</sup>J(H,P) = 3.6 Hz, 4H; –CH<sub>3</sub>); <sup>31</sup>P{<sup>1</sup>H} NMR (161.98 MHz, CDCl<sub>3</sub>, 25 °C, H<sub>3</sub>PO<sub>4</sub>): δ 10.3 (s).

**2b**: E.A. (%) calcd for C<sub>60</sub>H<sub>60</sub>N<sub>6</sub>Ag<sub>2</sub>P<sub>4</sub>S<sub>4</sub>: N, 6.30; C, 54.06; H, 4.54; S, 9.62. Found: N, 6.24; C, 54.41; H, 4.29; S, 9.55. <sup>1</sup>H NMR (300 MHz, CDCl<sub>3</sub>, 25 °C, TMS): δ = 7.0–7.5 (m, 20H; Ph), 3.78 (dq, <sup>3</sup>J(H,H) = 7.2 Hz, <sup>4</sup>J(H,P) = 4.2 Hz, 4H; –CH<sub>2</sub>–), 1.93 (t, 6H, <sup>3</sup>J(H,H) = 7.2 Hz; –CH<sub>3</sub>); <sup>31</sup>P{<sup>1</sup>H} NMR (161.98 MHz, CDCl<sub>3</sub>, 25 °C, H<sub>3</sub>PO<sub>4</sub>): δ 9.0 (s).

**Preparation of [Au(EtSNS)] (**3**)**. A solution of HEtSNS (112 mg, 0.2 mmol) in CH<sub>2</sub>Cl<sub>2</sub> (20 mL) was added to a solution of [(tht)AuCl] (64 mg, 0.2 mmol) in CH<sub>2</sub>Cl<sub>2</sub> (20 mL), resulting in a yellow reaction mixture. *t*-BuOK (22 mg, 0.2 mmol in 5 mL of MeOH) was in turn added, and stirring continued for 2 h. Evaporation of the solvent gave a pale yellow solid which was redissolved in CH<sub>2</sub>Cl<sub>2</sub> (20 mL). KCl was removed by filtration. Addition of hexane (10 mL) afforded a brown oil which was removed by centrifugation. Evaporation of the solvent yielded complex [Au(EtSNS)] (**3**) as a white powder. Yield: 83%.

E.A. (%) calcd for C<sub>30</sub>H<sub>30</sub>N<sub>3</sub>AuP<sub>2</sub>S<sub>2</sub>: N, 5.56; C, 47.69; H, 4.00; S, 8.49. Found: N, 5.34; C, 47.41; H, 4.19; S, 8.55. <sup>1</sup>H NMR (300 MHz, CDCl<sub>3</sub>, 25 °C, TMS): δ = 7.63–7.25 (m, 20H; Ph), 3.71 (dq, <sup>3</sup>J(H,H) = 7.2 Hz, <sup>4</sup>J(H,P) = 3.6 Hz, 4H; –CH<sub>2</sub>–), 1.21 (t, 6H, <sup>3</sup>J(H,H) = 7.2 Hz; –CH<sub>3</sub>). <sup>31</sup>P{<sup>1</sup>H} NMR (161.98 MHz, CDCl<sub>3</sub>, 25 °C, H<sub>3</sub>PO<sub>4</sub>): δ 10.9 (s).

**Preparation of [Cu<sub>2</sub>{Cu(RSNS)}<sub>3</sub>][PF<sub>6</sub>]<sub>2</sub> (R = Me, **4a**; R = Et, **4b**)**. (a) A solution of HRSNS (168 mg R = Et, 159 mg R = Me; 0.3 mmol) in CH<sub>2</sub>Cl<sub>2</sub> (15 mL) was added to a solution of [Cu(MeCN)<sub>4</sub>]-PF<sub>6</sub> (186 mg, 0.5 mmol) in CH<sub>2</sub>Cl<sub>2</sub> (15 mL), resulting in an orange reaction mixture. *t*-BuOK (34 mg, 0.3 mmol in 5 mL of MeOH) was in turn added, and stirring continued for 2 h. Evaporation of the solvent gave the crude product which was in turn recrystallized by evaporation from a CH<sub>2</sub>Cl<sub>2</sub>/hexane mixture, yielding complexes [Cu<sub>2</sub>{Cu(RSNS)}<sub>3</sub>]-

**Table 3.** Crystal Data and Structure Refinement for Complexes **1b**, **2a**, and **3**

complexes	<b>1b</b>	<b>2a</b>	<b>3</b>
formula	Cu <sub>2</sub> P <sub>2</sub> N <sub>3</sub> C <sub>30</sub> H <sub>30</sub>	Ag <sub>2</sub> S <sub>4</sub> P <sub>4</sub> N <sub>6</sub> C <sub>56</sub> H <sub>52</sub>	Au <sub>2</sub> P <sub>2</sub> N <sub>3</sub> C <sub>30</sub> H <sub>30</sub>
FW	622.17	1276.9	755.60
crystal system	monoclinic	monoclinic	monoclinic
space group	<i>C2/c</i>	<i>P2<sub>1</sub>/n</i>	<i>P2<sub>1</sub>/c</i>
<i>a</i> , Å	15.752(4)	20.776(6)	15.810(5)
<i>b</i> , Å	10.650(3)	14.173(4)	10.699(4)
<i>c</i> , Å	19.510(5)	21.317(6)	19.258(7)
α, deg	90	90	90
β, deg	113.16(5)	117.89(5)	113.459(8)
γ, deg	90	90	90
<i>V</i> , Å <sup>3</sup>	3009 (1)	5548(5)	2988(7)
<i>Z</i>	4	4	4
<i>D</i> <sup>calcd</sup> , g cm <sup>-3</sup>	1.373	1.529	1.680
<i>F</i> (000)	1288	2592	1488
crystal size (mm <sup>3</sup> )	0.23 × 0.17 × 0.12	0.20 × 0.09 × 0.15	0.54 × 0.45 × 0.20
μ, cm <sup>-1</sup>	9.95	10.15	51.95
rflns collected	15 546	43 169	6350
rflns unique	2661	7745	6173
rflns observed [ <i>I</i> > 2σ( <i>I</i> )]	1744	3726	3198
parameters	186	505	343
<i>R</i> indices	<i>R</i> 1 = 0.0395	<i>R</i> 1 = 0.0669	<i>R</i> 1 = 0.0418
[ <i>I</i> > 2σ( <i>I</i> )]	<i>wR</i> 2 = 0.0965	<i>wR</i> 2 = 0.1222	<i>wR</i> 2 = 0.482
<i>R</i> indices (all data)	<i>R</i> 2 = 0.0715	<i>R</i> 2 = 0.1421	<i>R</i> 2 = 0.1195
	<i>wR</i> 2 = 0.1059	<i>wR</i> 2 = 0.1368	<i>wR</i> 2 = 0.0551

[PF<sub>6</sub>]<sub>2</sub> (R = Me, Et; **4a** and **4b** respectively) as yellow crystalline solids. Yields: **4a** 81%, **4b** 83%.

(b) A solution of [Cu(MeCN)<sub>4</sub>]-PF<sub>6</sub> (74.5 mg, 0.2 mmol) in CH<sub>2</sub>Cl<sub>2</sub> (15 mL) was added to a solution of **1a** or **1b** (178 mg or 186 mg, respectively; 0.3 mmol) in CH<sub>2</sub>Cl<sub>2</sub> (15 mL), resulting in a yellow reaction mixture. Stirring was continued for 20 min. Evaporation of the solvent afforded clusters **4a** (from **1a**) and **4b** (from **1b**) as yellow crystalline powders. Yield: **4a** 92%, **4b** 96%.

**4a**: E.A. (%) calcd for C<sub>84</sub>H<sub>78</sub>N<sub>6</sub>Cu<sub>5</sub>F<sub>12</sub>P<sub>8</sub>S<sub>6</sub>: N, 5.73; C, 45.87; H, 3.57; S, 8.75. Found: N, 5.46; C, 44.65; H, 3.42; S, 8.24. <sup>1</sup>H NMR (300 MHz, CD<sub>2</sub>Cl<sub>2</sub>, 25 °C, TMS) δ = 7.7–7.1 (m, 60H; Ph), 3.72 (d, 18H, <sup>4</sup>J(H,P) = 3.6 Hz; –CH<sub>3</sub>). <sup>31</sup>P{<sup>1</sup>H} NMR (161.98 MHz, CDCl<sub>3</sub>, 25 °C, H<sub>3</sub>PO<sub>4</sub>): δ = 14.4 (s), –143.3 (sept, <sup>1</sup>J(P,F) = 711 Hz; PF<sub>6</sub>).

**4b**: E.A. (%) calcd for C<sub>90</sub>H<sub>90</sub>N<sub>6</sub>Cu<sub>5</sub>F<sub>12</sub>P<sub>8</sub>S<sub>6</sub>: N, 5.52; C, 47.34; H, 3.97; S, 8.42. Found: N, 5.36; C, 47.81; H, 4.09; S, 8.31. <sup>1</sup>H NMR (300 MHz, CD<sub>2</sub>Cl<sub>2</sub>, 25 °C, TMS): δ = 7.75–7.15 (m, 60H; Ph), 4.04 (m, br, 6H; –CHH–), 3.87 (m, br, 6H; –CHH–), 1.34 (t, 18H, <sup>3</sup>J(H,H) = 7.2 Hz; –CH<sub>3</sub>). <sup>31</sup>P{<sup>1</sup>H} NMR (161.98 MHz, CDCl<sub>3</sub>, 25 °C, H<sub>3</sub>-PO<sub>4</sub>): δ = 12.2 (s), –144.4 (sept, <sup>1</sup>J(P,F) = 712 Hz; PF<sub>6</sub>). ESI-MS [CH<sub>2</sub>Cl<sub>2</sub> solution; *m/z* (rel int., formula)]: 503.2 (5%, Ph<sub>2</sub>(S)PNPPh<sub>2</sub>-EtNCS<sup>+</sup>), 560.6 (5%, H<sub>2</sub>EtSNS<sup>+</sup>), 996.8 (100%, [Cu<sub>2</sub>{Cu(EtSNS)}<sub>3</sub>]<sup>2+</sup>, 1307.5 (2%, [Cu<sub>2</sub>{Cu(EtSNS)}<sub>4</sub>]<sup>2+</sup>).

**Preparation of [Ag<sub>2</sub>{Cu(RSNS)}<sub>3</sub>][A]<sub>2</sub> (R = Et, A = OTf<sup>-</sup> **5a**; R = Me, A = OTf<sup>-</sup> **5b**; R = Et, A = BF<sub>4</sub><sup>-</sup> **5c**)**. A solution of AgOTf (51 mg, 0.2 mmol) in THF (15 mL) was added to a solution of **1a** or **1b** (178 mg or 186 mg, respectively; 0.3 mmol) in CH<sub>2</sub>Cl<sub>2</sub> (15 mL), resulting in a yellow reaction mixture. Addition of hexane (30 mL) afforded clusters **5a** (from **1a**) and **5b** (from **1b**) as microcrystalline yellow powders. Yields: **5a** 87%, **5b** 93%. Cluster **5c** was prepared following the same procedure, using AgBF<sub>4</sub> (39 mg) instead of AgOTf and complex **1b** (178 mg). Yield: 90%.

**5a**: E.A. (%) calcd for C<sub>86</sub>H<sub>78</sub>N<sub>9</sub>Ag<sub>2</sub>Cu<sub>3</sub>F<sub>6</sub>O<sub>6</sub>P<sub>6</sub>S<sub>6</sub>: N, 5.49; C, 44.98; H, 3.42; S, 11.17. Found: N, 5.35; C, 45.44; H, 3.40; S, 10.96. <sup>1</sup>H NMR (300 MHz, CDCl<sub>3</sub>, 25 °C, TMS): δ = 7.6–7.3 (m, 60H; Ph), 3.72 (s, br, 18H; –CH<sub>3</sub>); <sup>31</sup>P{<sup>1</sup>H} NMR (161.98 MHz, CDCl<sub>3</sub>, 25 °C, H<sub>3</sub>PO<sub>4</sub>): δ = 16.3 (s).

**5b**: E.A. (%) calcd for C<sub>92</sub>H<sub>90</sub>N<sub>9</sub>Ag<sub>2</sub>Cu<sub>3</sub>F<sub>6</sub>O<sub>6</sub>P<sub>6</sub>S<sub>6</sub>: N, 5.30; C, 46.42; H, 3.81; S, 10.78. Found: N, 5.35; C, 46.34; H, 3.73; S, 10.64. <sup>1</sup>H NMR (300 MHz, CDCl<sub>3</sub>, 25 °C, TMS): δ = 7.60–7.26 (m, 60H; Ph), 3.85 (m, br, 12H; –CH<sub>2</sub>–), 1.31 (t, 18H; <sup>3</sup>J(H,H) = 7.2 Hz, –CH<sub>3</sub>).

**Table 4.** Crystal Data and Structure Refinement for Clusters **4a**, **5c**, **6a**, and **7**<sup>a</sup>

complexes	4a	5c	6a	7
formula	Cu <sub>5</sub> S <sub>6</sub> P <sub>6</sub> N <sub>9</sub> C <sub>84</sub> H <sub>78</sub> ·[PF <sub>6</sub> ] <sup>+</sup> 2CH <sub>2</sub> Cl <sub>2</sub> ·1/2MeOH	Cu <sub>3</sub> Ag <sub>2</sub> S <sub>6</sub> P <sub>6</sub> N <sub>9</sub> C <sub>90</sub> H <sub>90</sub> ·2BF <sub>4</sub>	Ag <sub>5</sub> S <sub>6</sub> P <sub>6</sub> N <sub>9</sub> C <sub>84</sub> H <sub>78</sub> · 2PF <sub>6</sub> ·4 toluene	Ag <sub>4</sub> S <sub>6</sub> P <sub>4</sub> O <sub>6</sub> C <sub>62</sub> F <sub>6</sub> H <sub>60</sub> · THF
FW	2385.23	2255.87	2605.26	1918.98
crystal system	monoclinic	hexagonal	monoclinic	monoclinic
space group	<i>P</i> 21/ <i>c</i>	<i>P</i> -3	<i>P</i> 21/ <i>c</i>	<i>P</i> 21/ <i>c</i>
<i>a</i> , Å	25.679(5)	17.955(5)	16.478(7)	15.701(7)
<i>b</i> , Å	14.502(5)	17.955(5)	26.693(6)	13.750(5)
<i>c</i> , Å	30.087(5)	17.601(4)	52.329(8)	17.964(6)
$\alpha$ , deg	90	90	90	90
$\beta$ , deg	109.262(5)	90	94.046(6)	98.935(9)
$\gamma$ , deg	90	120	90	90
<i>V</i> , Å <sup>3</sup>	10577(5)	4914(2)	22959(11)	3831(7)
<i>Z</i>	4	2	8	2
<i>D</i> <sub>calcd</sub> , g cm <sup>-3</sup>	1.497	1.525	1.507	1.663
<i>F</i> (000)	4820	2284	10 400	1904
crystal size (mm <sup>3</sup> )	0.34 × 0.21 × 0.19	0.23 × 0.32 × 0.24	0.52 × 0.34 × 0.33	0.18 × 0.51 × 0.39
$\mu$ , cm <sup>-1</sup>	13.97	13.19	11.24	13.22
rflns collect	45154	23970	95683	7302
rflns unique	14 699	5710	39 980	7079
rflns observed	7712	2647	11904	2639
[ <i>I</i> > 2 $\sigma$ ( <i>I</i> )]				
parameters	1228	319	1881	379
<i>R</i> indices	<i>R</i> 2 = 0.0567	<i>R</i> 2 = 0.0588	<i>R</i> 2 = 0.0566	<i>R</i> 2 = 0.0571
[ <i>I</i> > 2 $\sigma$ ( <i>I</i> )]	<i>wR</i> 2 = 0.1185	<i>wR</i> 2 = 0.1320	<i>wR</i> 2 = 0.1066	<i>wR</i> 2 = 0.0663
<i>R</i> indices	<i>R</i> 2 = 0.1331	<i>R</i> 2 = 0.1376	<i>R</i> 2 = 0.2004	<i>R</i> 2 = 0.1890
(all data)	<i>wR</i> 2 = 0.1389	<i>wR</i> 2 = 0.1433	<i>wR</i> 2 = 0.1203	<i>wR</i> 2 = 0.0809

$$^a RI = \sum ||F_o| - |F_c|| / \sum |F_o|. \quad wR2 = [\sum (w(F_o^2 - F_c^2)^2) / \sum (w(F_o^2)^2)]^{1/2}.$$

<sup>31</sup>P{<sup>1</sup>H} NMR (161.98 MHz, CDCl<sub>3</sub>, 25 °C, H<sub>3</sub>PO<sub>4</sub>):  $\delta$  = 13.2 (s). ESI-MS [CH<sub>2</sub>Cl<sub>2</sub> solution; *m/z* (rel int., formula)]: 996.8 (<1%, [Cu<sub>2</sub>{Cu(EtSNS)}<sub>3</sub>]<sup>2+</sup>), 1019.0 (3%, [Cu<sub>4</sub>Ag(EtSNS)<sub>3</sub>]<sup>2+</sup>), 1041.2 (100%, [Ag<sub>2</sub>{Cu(RSNS)}<sub>3</sub>]<sup>2+</sup>), 1063.3 (4%, [Cu<sub>2</sub>Ag<sub>3</sub>(EtSNS)<sub>3</sub>]<sup>2+</sup>), 1085.5 (<1%, [CuAg<sub>4</sub>(EtSNS)<sub>3</sub>]<sup>2+</sup>).

**5c**: E.A. (%) calcd for C<sub>90</sub>H<sub>90</sub>N<sub>9</sub>Ag<sub>5</sub>F<sub>6</sub>O<sub>6</sub>P<sub>6</sub>S<sub>6</sub>: N, 5.59; C, 47.92; H, 4.02; S, 8.52. Found: N, 5.73; C, 48.31; H, 3.99; S, 8.29. <sup>1</sup>H NMR (300 MHz, CDCl<sub>3</sub>, 25 °C, TMS):  $\delta$  = 7.8–7.3 (m, 60H; Ph), 3.86 (m, br, 12H; –CH<sub>2</sub>), 1.31 (t, 18H; <sup>3</sup>J(H,H) = 7.2 Hz, –CH<sub>3</sub>). <sup>31</sup>P{<sup>1</sup>H} NMR (161.98 MHz, CDCl<sub>3</sub>, 25 °C, H<sub>3</sub>PO<sub>4</sub>):  $\delta$  = 13.2 (s)

**Preparation of Clusters [Ag<sub>2</sub>{Ag(RSNS)}<sub>3</sub>][A]<sub>2</sub> (**6a**, R = Me, A = PF<sub>6</sub><sup>-</sup>; **6b**, R = Et, A = OTf<sup>-</sup>).** (a) A solution of AgOTf (51 mg, 0.2 mmol in 15 mL of THF) was added to a solution of complex **2b** (200 mg, 0.3 mmol, in 15 mL of THF). Stirring was continued for 10 min. Addition of hexane afforded cluster **6b** as a white powder, purified by crystallization from a CHCl<sub>3</sub>/hexane solution. Yield: 91%. Cluster **6a** was obtained following the same procedure, using AgPF<sub>6</sub> (51 mg) and complex **2a** (192 mg) instead of AgOTf and complex **2b**, respectively. Yield: 85%.

(b) A solution of AgOTf (128 mg, 0.5 mmol in 15 mL of THF) was added to a solution of HEtSNS (168 mg, 0.3 mmol, in 15 mL of THF). *t*-BuOK (34 mg, 0.3 mmol, in tot of MeOH) was in turn added, and stirring continued for 20 min. Evaporation of the solvent afforded a white solid which was redissolved in CH<sub>2</sub>Cl<sub>2</sub> (40 mL). KCl was removed by filtration. Evaporation of the solvent yielded cluster **6b** as a white powder. Yield: 73%. Cluster **6a** was obtained following the same procedure, using AgPF<sub>6</sub> (127 mg) and HMeSNS (159 mg) instead of AgOTf and HEtSNS, respectively. Yield: 69%.

(c) A solution of complex **2b** (133 mg, 0.2 mmol, in 15 mL of THF) was added to a solution of complex **7** (369 mg, 0.2 mmol, in 15 mL of THF). Stirring was continued for 10 min. Addition of hexane (40 mL) afforded cluster **6b** as a white powder, purified by crystallization from a CHCl<sub>3</sub>/hexane solution.

**6a**: E.A. (%) calcd for C<sub>90</sub>H<sub>90</sub>N<sub>9</sub>Ag<sub>5</sub>F<sub>12</sub>P<sub>6</sub>S<sub>6</sub>: N, 5.21; C, 41.67; H, 3.25; S, 7.95. Found: N, 5.03; C, 41.70; H, 3.42; S, 8.02. <sup>1</sup>H NMR (300 MHz, CDCl<sub>3</sub>, 25 °C, TMS):  $\delta$  = 7.2–7.45 (m, 60H; Ph), 3.47 (s, br, 18H; –CH<sub>3</sub>); <sup>31</sup>P{<sup>1</sup>H} NMR (161.98 MHz, CDCl<sub>3</sub>, 25 °C, H<sub>3</sub>PO<sub>4</sub>):  $\delta$  = 11.8 (s), –143.4 (sept, <sup>1</sup>J(P,F) = 712 Hz; PF<sub>6</sub><sup>-</sup>).

**6b**: E.A. (%) calcd for C<sub>92</sub>H<sub>90</sub>N<sub>9</sub>Ag<sub>5</sub>F<sub>6</sub>O<sub>6</sub>P<sub>6</sub>S<sub>6</sub>: N, 5.01; C, 43.96; H, 3.61; S, 10.21. Found: N, 5.32; C, 43.74; H, 3.84; S, 10.37. <sup>1</sup>H NMR (300 MHz, CDCl<sub>3</sub>, 25 °C, TMS):  $\delta$  = 7.7–7.5 (m, 60H; Ph), 3.97 (m, br, 12H; –CH<sub>2</sub>–), 1.43 (t, br, 18H; –CH<sub>3</sub>). <sup>31</sup>P{<sup>1</sup>H} NMR (161.98 MHz, CDCl<sub>3</sub>, 25 °C, H<sub>3</sub>PO<sub>4</sub>):  $\delta$  = 12.2 (s). ESI-MS [CH<sub>2</sub>Cl<sub>2</sub> solution; *m/z* (rel int., formula)]: 1066.1 (5%, [Ag<sub>2</sub>{Ag(EtSNS)}<sub>3</sub>]<sup>2+</sup> – EtNC), 1107.7 (100%, [Ag<sub>2</sub>{Ag(EtSNS)}<sub>3</sub>]<sup>2+</sup>).

**Preparation of Complex [Ag(EtSNS)]<sub>2</sub>{AgOTf}<sub>2</sub> (**7**).** (a) A solution of AgOTf (51 mg, 0.2 mmol in 15 mL of THF) was added to a solution of complex **2b** (133 mg, 0.2 mmol, in 15 mL of THF). Stirring was continued for 10 min. Addition of hexane resulted in the precipitation of complex **7** as a white powder, purified by crystallization from a THF solution.

(b) A solution of AgOTf (102 mg, 0.4 mmol in 15 mL of THF) was added to a solution of HEtSNS (104 mg, 0.2 mmol, in 15 mL of THF). *t*-BuOK was in turn added (22 mg, 0.2 mmol, in 5 of MeOH), and stirring continued for 20 min. Evaporation of the solvent afforded a white powder which was in turn redissolved in CH<sub>2</sub>Cl<sub>2</sub>. KCl was filtered. Evaporation of the solvent yielded complex **7** as a white powder.

E.A. (%) calcd for C<sub>62</sub>H<sub>60</sub>N<sub>6</sub>Ag<sub>4</sub>F<sub>6</sub>O<sub>6</sub>P<sub>4</sub>S<sub>6</sub>: N, 4.55; C, 40.32; H, 3.27; S, 10.42. Found: N, 4.73; C, 40.51; H, 3.56; S, 10.56. <sup>1</sup>H NMR (300 MHz, CDCl<sub>3</sub>, 25 °C, TMS):  $\delta$  = 7.7–7.2 (m, 40H; Ph), 3.97 (m, br, 8H; –CH<sub>2</sub>–), 1.29 (t, br, 12H; –CH<sub>3</sub>). <sup>31</sup>P{<sup>1</sup>H} NMR (161.98 MHz, CDCl<sub>3</sub>, 25 °C, H<sub>3</sub>PO<sub>4</sub>):  $\delta$  = 14.6 (s). ESI-MS [CH<sub>2</sub>Cl<sub>2</sub> solution; *m/z* (rel int., formula)]: 1107.7 (12%, [Ag<sub>2</sub>{Ag(EtSNS)}<sub>3</sub>]<sup>2+</sup>), 1697.9 (100%, [Ag<sub>2</sub>{Ag(EtSNS)}<sub>2</sub>OTf]<sup>+</sup>).

**X-ray Data Collection, Structure Solution, and Refinement for Compounds 1b, 2a, 3, 4a, 5c, 6a, and 7.** Suitable crystals for the X-ray analysis for complexes **1b**, **2a**, **3b** were obtained by layering hexane on dichloromethane solutions, for cluster **4a** by evaporation of a CH<sub>2</sub>Cl<sub>2</sub>/MeOH solution, for **5c** by evaporation of a CH<sub>3</sub>Cl/hexane solution, for cluster **6a** by evaporation of a toluene/CH<sub>2</sub>Cl<sub>2</sub> solution and for cluster **7** by evaporation of a THF solution. The intensity data were collected at room temperature on a Bruker area detector AXS Smart 1000<sup>25</sup> [**1b**, **2a**, **4a**, **5c**, **6a**] and on a Philips PW 1100 (**3** and **7**) single-crystal diffractometer (using a graphite monochromated Mo K $\alpha$  radiation,  $\lambda$  = 0.710 73 Å, for both). Crystallographic and experimental

details for the structures are summarized in Tables 3 and 4. Bruker SADABS software<sup>26</sup> [**1b**, **2a**, **4a**, **5c**, **6a**; maximum and minimum transmission coefficient values: 1.000 and 0.788 (**1b**), 1.000 and 0.586 (**2a**), 1.000 and 0.680 (**4a**), 1.000 and 0.741 (**5c**), 1.000 and 0.946 (**6a**), and psi-scan methods<sup>27</sup> [**3** and **7**, maximum and minimum transmission coefficient values: 1.000 and 0.388, 1.000 and 0.610, respectively] were used for the absorption correction. The structures were solved by direct methods and refined by full-matrix least-squares procedures (based on  $F_o^2$ , SHELX-97)<sup>28</sup> first with isotropic thermal parameters and then with anisotropic thermal parameters in the last cycles of refinement for all the non-hydrogen, except those of the solvent molecules for **6a**. The hydrogen atoms were introduced into the geometrically calculated positions and refined *riding* on the corresponding parent atoms, except those bound to solvent molecules. In **2a** the ethyl groups were found disordered in two positions with equal occupancy factors. CCDC-256438 (**1b**), CCDC-280044 (**2a**), CCDC-

280045 (**3**), CCDC-256439 (**4a**), CCDC-280046 (**5c**), CCDC-280047 (**6a**), and CCDC-280048 (**7**) contain the supplementary crystallographic data for this paper that can be obtained free of charge from the Cambridge Crystallographic Data Centre via [www.ccdc.cam.ac.uk/data\\_request/cif](http://www.ccdc.cam.ac.uk/data_request/cif). The CIF files are also included in the Supporting Information.

**Acknowledgment.** We thank Dr. Efstathia E. Sakellariou (National Chemistry Lab., Athens, Greece) for the help in preparing the manuscript; Dr. Enrico Cavalli (Dipartimento di Chimica Generale ed Inorganica, Chimica Analitica, Chimica Fisica, University of Parma, Italy) for the collection of the emission spectra of complex **4b**, and Ministero dell'Istruzione, dell'Università e della Ricerca for financial support.

**Supporting Information Available:** X-ray crystallographic data in CIF format; Ortep diagrams with thermal ellipsoids; a discussion of the HMeSNS and H<sub>2</sub>MeSNS <sup>1</sup>H NMR spectra; the emission spectra of cluster **4a** and a series of <sup>1</sup>H NMR spectra recorded in the temperature range 298–230 K. This material is available free of charge via the Internet at <http://pubs.acs.org>.

JA0554110

(25) Sheldrick, G. M. *SADABS*; Bruker Analytical X-ray Systems, Madison, WI, 1999.

(26) *SAINT Software Users Guide; SMART Software Users Guide*; Bruker Analytical X-ray Systems: Madison, WI, 1999.

(27) Ugozzoli, F. DIFAU-92.

(28) Sheldrick, M. *SHELXL-97*, Program for crystal structure refinement; University of Göttingen: Germany, 1997.